Available online at www.sciencedirect.com
ScienceDirect
Trans. Nonferrous Met. Soc. China 28(2018) 2335−2341

Transactions of Nonferrous Metals Society of China
www.tnmsc.cn

Effects of $BaCl_2$ on K-feldspar flotation using dodecyl amine chloride under natural pH

Chao SONG[1], Yuan-yuan ZHOU[1,2], Quan-jun LIU[1], Jian-ying DENG[1], Shi-mei LI[1], Li-kun GAO[1], Li YU[1]

1. State Key Laboratory of Complex Nonferrous Metal Resources Clean Utilization,
Faculty of Land Resource Engineering, Kunming University of Science and Technology, Kunming 650093, China;
2. Henan Key Laboratory of Aeronautical Materials and Application Technology,
School of Mechatronics Engineering, Zhengzhou University of Aeronautics, Zhengzhou 450046, China

Received 9 September 2017; accepted 15 March 2018

Abstract: The effects of $BaCl_2$ on the flotation of K-feldspar using dodecyl amine chloride as the collector under natural pH were investigated by flotation tests, absorption measurements, Fourier transform infrared spectroscopy (FTIR) and X-ray photoelectron spectroscopy (XPS). The results indicated that lower $BaCl_2$ concentration can increase the floatability of K-feldspar, whereas higher $BaCl_2$ concentration can significantly inhibit the flotation of K-feldspar. Peaks at 3548.18, 3475.56 and 3414.35 cm^{-1} in the FTIR spectra of K-feldspar adsorbed by dodecyl amine chloride revealed three forms of —OH. XPS analyses of K-feldspar adsorbed by Ba^{2+} showed that the concentration of K atom was reduced by nearly twice as those of Si, Al, and O. The activation of $BaCl_2$ at a low concentration was mainly caused by Ba^{2+} in the form of the ion exchange between K^+ and Ba^{2+}. The inhibitory action of $BaCl_2$ at a high concentration is mainly attributed to the physical absorption of Ba^{2+} on the surface of K-feldspar and the fact that a high concentration of Cl^- causes the chemical equilibrium of dodecyl amine chloride to be changed, and the dodecyl amine chloride in the form of RNH_2H^+ is reduced.

Key words: K-feldspar; $BaCl_2$; dodecyl amine chloride; activation; flotation

---

1 Introduction

K-feldspar is a type of feldspar mineral with a main chemical composition of K_2O, SiO_2, and Al_2O_3. A significant amount of K-feldspar is used in the glass and ceramics industries [1]. The quality of K-feldspar is mainly determined by the colored impurities, the quartz, and the ratio of K_2O/Na_2O (percentage composition) [2]. Flotation is the most commonly used method for feldspar separation. It is also the only means to increase the ratio of K_2O/Na_2O.

Numerous studies were focused on the effects and interaction mechanism of various ions on the flotation of minerals [3−5]. Metallic ions such as Fe^{3+} and Ca^{2+} effectively activate the flotation of spodumene and beryl. FTIR analysis suggested that the activation mechanism of Fe^{3+} involves the chemical absorption of the collector onto the surface of Fe^{3+}-activated mineral. Fe^{3+} can be activated in the flotation of spodumene, albite, and quartz [6]. The adsorption of Fe^{3+} onto the surface of spodumene, albite, and quartz can unexpectedly increase the amount of sodium oleate collector, and Fe^{3+} can switch the surface of these minerals from polar to non-polar [7,8]. The effect of Pb^{2+} ions on the flotation of ilmenite was researched, the pH had an influence on the form of Pb^{2+} and the adsorption of Pb^{2+} influenced the zeta potential and the number of activated sites on the mineral surface [9].

Activator is a general term for flotation reagents, which can be classified as organic or inorganic [10−12]. The inorganic reagent $BaCl_2$ was used in the present research. Ions with similar atomic radii, such as Ba, Rb, and Cs, can be used to depress the flotation of K-feldspar [13]. The adsorption and ion exchange of bivalent ions on the surface of feldspar were complex, and the selective separation of albite from microcline was achieved by micro-flotation with $CaCl_2$ and $BaCl_2$ as the regulators and amine (G-TAP) as the collector [14].

FTIR studies on the effects of Ca^{2+} and Mg^{2+} on the

Foundation item: Project (51764021) supported by the Key Program of the National Natural Science Foundation of China
Corresponding author: Quan-jun LIU; Tel: +86-13888860387; E-mail: kmliuqj@sina.com
DOI: 10.1016/S1003-6326(18)64878-2

flotation of spodumene showed that the surface change of spodumene through the absorption of hydroxyl complexes and precipitates promotes oleate complex formation, collector adsorption and mineral flotation [15]. Clay minerals have been studied using FTIR spectroscopy, suggesting that this method can be used to obtain fundamental information on the chemical composition, surface properties, and structural changes of minerals and their effects. The adsorption of organo-cations on montmorillonite in montmorillonite-water systems has also been investigated [16−18]. The adsorption mechanism of dodecyl ammine on the surface of calcite was researched by FTIR, and the conclusion that sodium carbonate decreases the negative charges on the surface of calcite mineral was confirmed [19].

The addition of ions changes the surface properties of minerals, and XPS analysis was used to study these changes. The mechanism underlying the adsorption of mixed dithiophosphate and mercaptobenzothiazole on the surface of copper sulfide ore has been investigated using XPS [20,21]. Results have proven that the F chemistry from $LiPF_6$ is the major difference among various coatings, and that the reaction mechanism occurring on the metal oxide surface has been ascertained according to the change in potentials [22,23]. The adsorption mechanisms of organic reagent on mineral surface were also researched by XPS. The adsorption mechanisms of disodium bis (carboxymethyl) trithiocarbonate on the surface of chalcopyrite was researched by using XPS [24].

New methods of feldspar separation were also reported. Hydrofluoric acid (HF) was used in the separation of quartz and feldspar, thus high grades and good recoveries were obtained [25]. Cyclojet flotation cell was used in the beneficiation of low-grade feldspar. The result shows that with cyclojet flotation cell, both Fe_2O_3 and TiO_2 can be removed at a rate of up to 90%, and much better than magnetic separator [26].

The present study aimed to determine the influence of $BaCl_2$ on the flotation of K-feldspar with dodecyl amine chloride, and explained the underlying mechanism through FTIR and XPS analyses of solution and surface chemistries.

2 Experimental

2.1 Materials

High-purity K-feldspar samples were obtained from Shandong Province, China. The chemical composition of the samples is presented in Table 1. The lump-sized materials were crushed with a hammer and ground in an agate mortar followed by dry screening to produce samples (d_{80}=56 μm) for the flotation and XPS studies and the adsorption experiments. The specific surface area for the size fractions of the K-feldspar samples was 0.379 m^2/g.

Table 1 Chemical composition of K-feldspar (mass fraction, %)

K_2O	Na_2O	SiO_2	Al_2O_3	Fe_2O_3	Others
13.15	1.80	64.84	17.89	0.017	2.303

2.2 Reagents

Dodecyl amine chloride was synthesized in the laboratory under 25 °C by lauryl amine and hydrochloric with a molecular proportion of 1:1. Barium chloride dehydrate was supplied by Ruijinte Chemicals Co., Ltd., China.

2.3 Flotation tests

Single mineral flotation tests were performed in a 50 mL flotation cell with a mechanical agitator. A flotation test sample (d_{80}=56 μm) of approximately 2 g was mixed with 50 mL of deionized water (including the reagent volume) at an impeller speed of 1600 r/min. Conditioning and flotation were performed at the same impeller speed and pulp volume. Firstly, 2.0 g of the mineral sample was conditioned in deionized water for 2 min with stirring. Barium chloride dehydrate was used as a regulator and conditioned for 3 min. Then, dodecyl amine chloride was conditioned for 3 min. The optimum flotation time of 2 min was used in all flotation tests. The concentrate and tailing were dried separately at 35 °C and weighed to calculate the productivity and recovery.

2.4 Adsorption experiments

Adsorption experiments of Ba^{2+} from solution onto the surface of K-feldspar were performed in a beaker. For each experiment, 4 g of powder sample and 40 mL working solution with a specific $BaCl_2$ concentration were added into a 100 mL beaker, and the suspension was conditioned for 30 min. After centrifugation, the $BaCl_2$ concentration of the water phase was determined by ICP-MS (UV). The adsorption of $BaCl_2$ onto the material was calculated as the difference between the initial and final $BaCl_2$ concentrations of water [27].

2.5 FTIR spectral analysis

The infrared spectra FTIR measurements were performed with 50 mL suspension containing 2 g powder sample and 50 mL water which was conditioned for 2 min. The suspension was added with 1.1×10^{-2} mol/L $BaCl_2$ and then conditioned for 3 min. Finally, the suspension was added with 10 mg/L dodecyl amine chloride and then conditioned for 3 min, and the samples were air-dried after filtration. FTIR spectra were obtained with a Nicolet iS10 FTIR spectrometer with its own attachment, and the average spectrum was 200 scans at 4 cm^{-1} resolution with a liquid nitrogen-cooled MCT detector. About 25 mg of the air-dried sample was mixed with 125 mg of KBr [28] and then tableted by a sheeter. The untreated K-feldspar powder was used as reference and the absorbance units were defined by the decimal logarithm of the ratio of initial K-feldspar reflectance to that of the sample. The atmospheric water was subtracted from the sample spectrum.

2.6 XPS analyses

Approximately 1.0 g of feldspar powder sample was conditioned in 40 mL of water for 25 min with $BaCl_2$ concentration of 1.1×10^{-2} and 5.3×10^{-2} mol/L. The XPS studies were performed on a PHI 5000 Versaprobe-II scanning XPS microprobe system with a mono-irradiation Al X-ray source of 50 W. Each analysis started with a survey scan from 0 to 1100 eV and pass energy of 46.95 eV. A value of 284.8 eV was adopted as the standard C1s binding energy [29,30].

3 Results and discussion

3.1 Flotation and adsorption tests

The flotation experiments were performed with K-feldspar using dodecyl amine chloride to determine the influence of $BaCl_2$ on the flotation of K-feldspar. The experiments were performed under the following conditions: pH 7.8, 2 min of mixing time, 1600 r/min of stirring rate, 10 mg/L of dodecyl amine chloride concentration, and 2 min of rising time. The only variable is the amount of $BaCl_2$. Figure 1 shows the flotation results of K-feldspar at different $BaCl_2$ concentrations, and the effect of $BaCl_2$ concentration on the adsorption capacity of Ba^{2+} on the surface of K-feldspar.

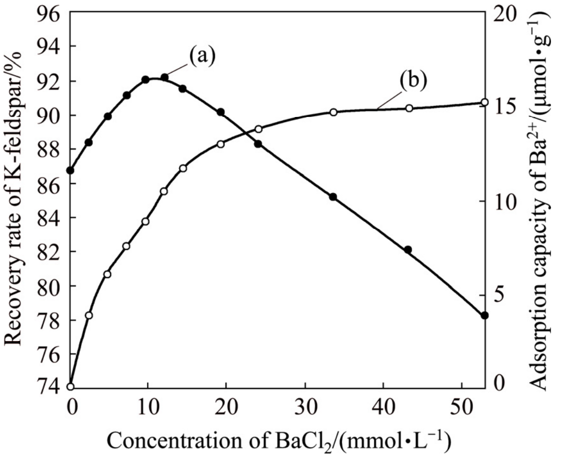

Fig. 1 Recovery rate of K-feldspar versus $BaCl_2$ concentration at 10 mg/L of dodecyl amine chloride addition (a) and effect of $BaCl_2$ concentration on adsorption capacity of Ba^{2+} on surface of K-feldspar (b)

As shown in Fig. 1(a), the recovery rate of K-feldspar was obtained at natural pH as a function of reagent dosage. The results indicated that the recovery rate of K-feldspar increased with increasing dosage when the concentration of $BaCl_2$ was lower than 1.1×10^{-2} mol/L. The recovery rate of K-feldspar increased from 86.73% to 92.21% (nearly 5%) when the $BaCl_2$ concentration was increased from 0 to 1.1×10^{-2} mol/L. However, the recovery rate of K-feldspar decreased with increasing dosage when the concentration of $BaCl_2$ exceeded 1.1×10^{-2} mol/L. The recovery rate of K-feldspar declined from 97.27% to 84.5% (nearly 13%) when $BaCl_2$ concentration was increased from 1.1×10^{-2} to 5.3×10^{-2} mol/L.

The results of flotation tests indicated that the $BaCl_2$ concentrations exerted a distinct influence on the flotation of K-feldspar using dodecyl amine chloride as the collector. In specific, low $BaCl_2$ concentration activated the flotation of K-feldspar, whereas high $BaCl_2$ concentration inhibited this process.

As shown in Fig. 1(b), the adsorption capacity of Ba^{2+} on the surface of K-feldspar increased throughout the test range of $BaCl_2$ concentration. The adsorption capacity of Ba^{2+} can be divided into three stages. The first stage is the rapid rise stage, which occurs when the concentration of $BaCl_2$ is less than 7.2×10^{-3} mol/L. In this stage, the adsorption capacity of Ba^{2+} increased from 0 to 7.6×10^{-3} mol/g. The second stage is the steady rise stage, which occurs when the concentration of $BaCl_2$ is greater than 7.2×10^{-3} mol/L and less than 2.1×10^{-2} mol/L. In this stage, the adsorption capacity of Ba^{2+} increased from 7.6×10^{-3} to 1.3×10^{-2} mol/g. The third stage is the slow rise stage, which occurs when the concentration of $BaCl_2$ exceeds 2.1×10^{-2} mol/L. In this stage, the adsorption capacity of Ba^{2+} approached the saturation state, after which the adsorption capacity of Ba^{2+} increased very slowly.

Figures 1(a) and (b) were compared, and the following results were obtained. In the rapid rise stage of the adsorption capacity of Ba^{2+}, the recovery rate of K-feldspar increased with the increase of the adsorption capacity of Ba^{2+}. In the steady rise stage, the recovery rate of K-feldspar initially increased and then decreased. However, the recovery rate exceeded 90% and was in the narrow fluctuation range. In the slow rise stage, the recovery rate of K-feldspar decreased as the adsorption capacity of Ba^{2+} increased.

3.2 FTIR spectral analysis

The FTIR absorption bands in the K-feldspar tests were mainly Si—O and Al—O groups, and the range of feldspar spectra was mainly 1200−300 cm^{-1}. The FTIR spectra of K-feldspar, the K-feldspar reaction with dodecyl amine chloride, and the K-feldspar reaction with dodecyl amine chloride after addition of $BaCl_2$ are shown in Fig. 2.

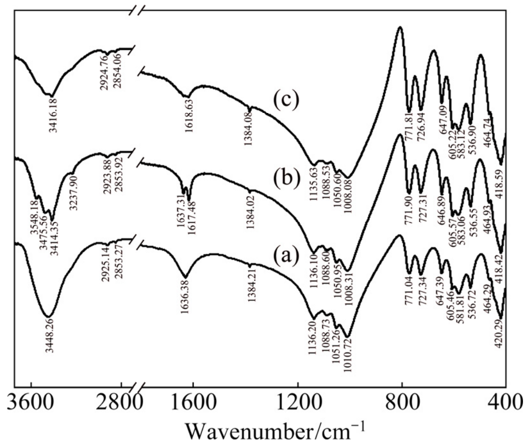

Fig. 2 FTIR spectra of K-feldspar (a), K-feldspar + dodecyl amine chloride (b) and K-feldspar + $BaCl_2$ + dodecyl amine chloride (c)

Figure 2 indicates that the peaks of spectra (b) and (c) are significantly lower than that of spectrum (a) at about 1051, 1010, and 420 cm^{-1}. This figure also shows a noticeable increase in the wavenumber at about 581 cm^{-1}. The peak at about 1051 cm^{-1} was attributed to the stretching vibration of Si—O groups, that at about 1010 cm^{-1} was attributed to Si(Al)—O groups, that at about 581 cm^{-1} was attributed to the bending vibration of O—Si(Al)—O groups, and that at about 420 cm was attributed to the bending vibration of Si—O—Si groups. The wavenumber decreases with the enhancement of Al—O groups, but it increases with the enhancement of Si—O groups [31].

The FTIR spectra in Fig. 2 at 400−1250 cm^{-1} confirm that dodecyl amine chloride as the collector can alter the peaks of K-feldspar, indicating that the chemical bonds of the mineral surface have been influenced. The peak at 1010.72 cm^{-1} which belongs to the stretching vibration of Si(Al)—O in Fig. 2(a) reduced to the peak at 1008.31 cm^{-1} in Fig. 2(b). The peak at 581.81 cm^{-1} which belongs to the bending vibration of O—Si(Al)—O in Fig. 2(a) increased to the peak at 583.06 cm^{-1} in Fig. 2(b). The displacement of the wavenumber indicates that the combined capacities of the Si and O atoms are reduced and the influence of the Al atom is enhanced, proving that dodecyl amine chloride interacts with the mineral surface and reduces the electronegativity of the Si atom.

The FTIR spectra of samples in the wavenumber range of 1250−4000 cm^{-1} in Fig. 2 show that the spectra (a), (b), and (c) changed significantly at about 3500 and 1630 cm^{-1}, and a new characteristic peak appeared at 3237.90 cm^{-1}. The peak at 3448.26 cm^{-1} in Fig. 2(a) was split into peaks at 3414.35, 3475.56 and 3548.18 cm^{-1} in Fig. 2(b); the peak at 1636.38 cm^{-1} in Fig. 2(a) was split into peaks at 1617.48 and 1637.31 cm^{-1} in Fig. 2(b). The peaks at 3448.26 cm^{-1} and 1636.38 cm^{-1} were attributed to the stretching and bending vibrations of O—H groups, respectively. Their split indicated the presence of three O—H groups on the mineral surface after the treatment with dodecyl amine chloride.

On the surface of K-feldspar exposed to the Si, O, and Al atoms, K$^+$ was mostly dissolved in the pulp. The O atoms on the mineral surface can be classified into two categories, namely, terminal (>Si—O—), which can be combined with H$^+$ from water to form >Si—OH, and bridging >Si—O—Si< and >Al—O—Si<, which can be combined with H_2O by the H-bond. The >Si$^+$ on the surface can combine with the —OH to form ≡Si—OH and with H_2O by H-bond vaporization in the drying process, and only one type of —OH can be detected by FTIR. Four forms of dodecyl amine chloride appeared in the solution: RNH_3^+, $RNH_2\cdot RNH_3^+$, $(RNH^{3+})_2^{2+}$, and RNH_2(aq) at pH 7−8. Reportedly, >AlO$^-$, >AlOH, > $AlOH_2^+$, >SiO$^-$, >SiOH, and > $SiOH_2^+$ groups exist in water [32]. The combination mode of amine on the mineral surface can be expressed as follows: (1) RNH_3^+ combined with terminal O atom by the formation of —OH and H-bond; (2) RNH_3^+ combined with the bridging O between Si and Al atoms by the formation of —OH and H-bond, and (3) RNH_2 combined with the bridging O atom between the Si atoms by the H-bond.

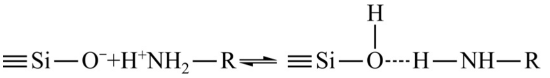
$$\equiv \mathrm{Si{-}O^-} + \mathrm{H^+NH_2{-}R} \rightleftharpoons \equiv \mathrm{Si{-}\overset{\overset{\textstyle H}{|}}{O}\cdots H{-}NH{-}R} \tag{1}$$

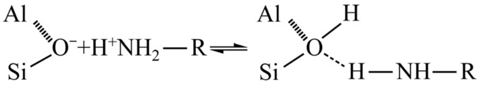
$$\mathrm{(Al)(Si)O^-} + \mathrm{H^+NH_2{-}R} \rightleftharpoons \mathrm{(Al)(Si)O(H)\cdots H{-}NH{-}R} \tag{2}$$

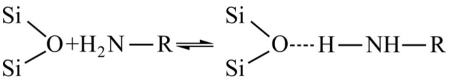
$$\mathrm{(Si)_2O} + \mathrm{H_2N{-}R} \rightleftharpoons \mathrm{(Si)_2O\cdots H{-}NH{-}R} \tag{3}$$

Dodecyl amine chloride adsorption onto the surface of K-feldspar with three types of adsorption modes produced three peaks of stretching vibration of —OH groups and two peaks of bending vibration of —OH in Fig. 2(b). The peak at 3548.18 cm^{-1} was attributed to the stretching vibration of >Si—OH—Al< groups [33], the peak at 3475.56 cm^{-1} was attributed to the stretching vibration of >Si—OH—Si< groups, and the peak at 3414.35 cm^{-1} was attributed to the stretching vibration of H-bond between the O atom of the mineral and the H atom of amine. The peak at 1637.31 cm^{-1} was attributed to the bending vibration of >Si—OH groups, and 1617.48 cm^{-1} was attributed to the bending vibration of >Si—OH—Al< groups. The peak at 3237.90 cm^{-1} was attributed to the N—H groups of dodecyl amine.

The spectrum in Fig. 2(c) is considerably different from that in Fig. 2(b), proving an obvious effect of $BaCl_2$ on the adsorption of dodecyl amine onto the surface of K-feldspar. The peaks of —OH in Fig. 2(c) were simpler than those in Fig. 2(b) (only 3416.18 cm^{-1}), which can be attributed to the stretching vibration of the H-bond between the O atom of the mineral and the H atom of amine, and the bending vibration of —OH was obviously lower in Fig. 2(c) than that in Fig. 2(b). The peak of the N—H group was not found in Fig. 2(c). Thus, when $BaCl_2$ acted as an inhibitor, the adsorption of RNH_3^+ onto the mineral surface with a covalent bond was more sensitive than that of RNH_2 with H-bond.

3.3 XPS analysis

XPS analysis was used to study the effect of $BaCl_2$ on the surface of K-feldspar. The XPS spectra are presented in Fig. 3, and the change of atoms in mole fraction on the mineral surface is provided in Table 2.

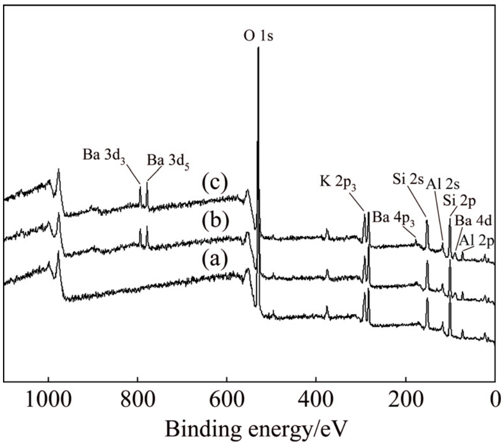

Fig. 3 XPS spectra of K-feldspar in the absence and presence of $BaCl_2$ on natural pH, respectively: (a) K-feldspar leaching with pure water for 25 min; (b) K-feldspar leaching with 1.1×10^{-2} mol/L $BaCl_2$ dehydrated solution for 25 min; (c) K-feldspar leaching with 4.8×10^{-2} mol/L $BaCl_2$ dehydrated solution for 25 min

Table 2 Mole fractions of atoms on mineral surface and their proportional shift

Sample No.	Mole fraction/%				
	O	Al	Si	K	Ba
a	73.33	2.51	14.58	9.58	–
b	67.57	2.36	13.32	8.01	8.74
c	67.19	2.42	13.29	8.13	8.97

Sample No.	Proportional shift/%				
	O	Al	Si	K	Ba
a	–	–	–	–	–
b	−7.85	−5.98	−8.64	−16.39	–
c	−8.37	−3.59	−8.85	−15.14	2.63

Figure 3 confirms that $BaCl_2$ can be adsorbed on the surface of K-feldspar with a chemical bond. The mole fractions in Table 2 indicate that mole fraction of Ba^{2+} was increased by 2.63% when $BaCl_2$ concentration was increased from 1.1×10^{-2} to 4.8×10^{-2} mol/L. The adsorption result in Fig. 1 shows that $BaCl_2$ was adsorbed on the mineral surface. According to the XPS spectra in Fig. 3, it can be confirmed that Ba^{2+} can be adsorbed on the mineral surface through chemisorption when the $BaCl_2$ concentration was lower than 1.1×10^{-2} mol/L. Table 2 shows that the mole fraction of Ba on mineral surface changed from 8.74% to 8.97% when the $BaCl_2$ concentration was increased from 1.1×10^{-2} to 4.8×10^{-2} mol/L. In consideration of the adsorption result in Fig. 1, it can be speculated that the Ba^{2+} adsorbed onto the mineral surface mainly through physical adsorption when $BaCl_2$ concentration exceeded 1.1×10^{-2} mol/L.

The proportional shift in Table 2 confirms that the shift rate of K was more obvious than that of O, Al and Si. The frame structure of K-feldspar under the ideal condition is illustrated in Fig. 4. K^+ entered the skeleton as counterbalance ion and was easily diffused into the pulp. Ba^{2+} had a similar ionic radius to K^+ and easily entered into the crystal skeleton by filling the vacancy caused by the dissolution of K^+. The positron of Ba^{2+} was twice that of K^+. Thus, the adjacent crystal lattice had no more need for extra positron from K^+, and the shift rate of K^+ became nearly twice those of the other atoms.

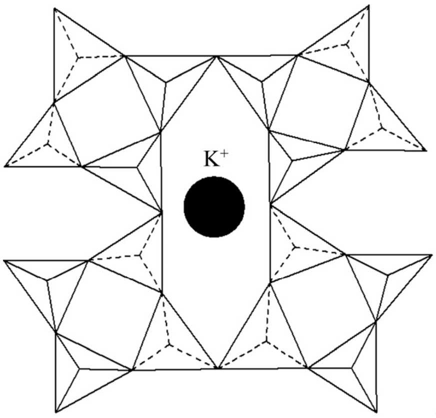

Fig. 4 Framework structure of idealized K-feldspar

The FTIR and XPS spectral analyses of the flotation mechanism can be explained as follows. The activation of $BaCl_2$ at a low concentration was caused by the ion exchange on the mineral surface, and the replacement of K^+ by Ba^{2+} increased the lattice vacancies and adsorption sites on the mineral surface [34]. With the increase in $BaCl_2$ concentration, the balance of ion exchange was achieved, Ba^{2+} adsorbed on the mineral surface by chemisorption reached the maximum, and maximum recovery rate of K-feldspar was reached. Subsequently, some of the adsorption sites were covered by Ba^{2+} adsorbed on the mineral surface and hindered the adsorption of dodecyl amine chloride with the continuous increase in concentration. The dissociation equilibrium of dodecyl amine chloride existed in the pulp, as shown by Eq. (4). The concentration of Cl^- increased with increasing $BaCl_2$ concentration, and the equilibrium moved to the left, which means that the concentration of RNH_3^+ decreased and the concentration of the collector with reactivity increased.

$$RNH_2{\cdot}HCl \rightleftharpoons RNH_3^+ + Cl^- \tag{4}$$

The ion exchange adsorption, physical absorption, and chemical equilibrium in the pulp are the main influencing factors of K-feldspar flotation with $BaCl_2$ as the regulator and dodecyl amine chloride as the collector.

4 Conclusions

1) The flotation of K-feldspar with $BaCl_2$ and dodecyl amine chloride shows that within the scope of the test $BaCl_2$ concentration, the recovery rate of K-feldspar increases with the increase of the $BaCl_2$ concentration when it is below 1.1×10^{-2} mol/L, and decreases with the increase of the $BaCl_2$ concentration when it is beyond 1.1×10^{-2} mol/L.

2) Dodecyl amine chloride is adsorbed on the surface of K-feldspar with three forms and causes three peaks at 3548.18, 3475.56, and 3414.35 cm^{-1}.

3) The ion exchange between K^+ and Ba^{2+} is a major factor of the low concentration of $BaCl_2$ and promotes the flotation of K-feldspar. The physical absorption of Ba^{2+} increases with the increase of the concentration of $BaCl_2$ when the concentration of $BaCl_2$ exceeds 1.3×10^{-2} mol/L, and the physical absorption becomes a major influencing factor of flotation. The chemical equilibrium of dodecyl amine chloride ionization form $RNH_2{\cdot}HCl$ increased and also had some impact on the inhibition of K-feldspar flotation.

References

[1] GULGONUL I, KARAGUZEL C, CELIK M S. Surface vs bulk analyses of various feldspars and their significance to flotation[J]. International Journal of Mineral Processing, 2008, 86: 68−74.

[2] KARAGUZEL C, GULGONUL I, DEMIR C, CELIK M S. Concentration of K-feldspar from a pegmatitic feldspar ore by flotation [J]. International Journal of Mineral Processing, 2006, 81: 122−132.

[3] DENG Jiu-shuai, LEI Yan-hua, WEN Shu-ming, CHEN Zhao-xu. Modeling interactions between ethyl xanthate and Cu/Fe ions using DFT/B3LYP approach [J]. International Journal of Mineral Processing, 2015, 140: 43−49.

[4] DENG Jiu-shuai, MAO Ying-bo, WEN Shu-ming, XIAN Yong-jun, LIU Jian. A new influencing factor inducing difficulty in selective flotation separation of Cu−Zn mixed sulphide minerals [J]. International Journal of Minerals, Metallurgy and Materials, 2015, 22: 111−116.

[5] JIANG H R, WU M C, ZHOU X L, YAN X H, ZHAO T S. Computational insights into the effect of carbon structures at the atomic level for non-aqueous sodium−oxygen batteries [J]. Journal of Power Sources, 2016, 325: 91−97.

[6] WANG Yu-hua, YU Fu-shun. Effects of metallic ions on the flotation of spodumene and beryl [J]. International Journal of Mining Science and Technology, 2007, 17(1): 35−39

[7] ZHANG Jie, WANG Wei-qing, LIU Jing, HUANG Yang, FENG Qi-ming, ZHAO Hong. Fe(III) as an activator for the flotation of spodumene, albite, and quartz minerals [J]. Minerals Engineering, 2014, 61: 16−22.

[8] CHEN H Y, RUCKENSTEIN E. Nanomembrane containing a nanopore in an electrolyte solution: A molecular dynamics approach [J]. The Journal of Physical Chemistry Letters, 2014, 5: 2979−2982.

[9] XU Long-hua, TIAN Jia, WU Hou-qin, LU Zhong-yuan, YANG Yao-hui, SUN Wei, HU Yue-hua. Effect of Pb^{2+} ions on ilmenite flotation and adsorption of benzohydroxamic acid as a collector [J]. Applied Surface Science, 2017, 425: 796−802.

[10] DENG J S, WEN S M, LIU J, WU D D, FENG Q C. Adsorption and activation of copper ions on chalcopyrite surfaces: A new viewpoint of self-activation [J]. Transactions of Nonferrous Metals Society of China, 2014, 24: 3955−3963.

[11] DENG Jiu-shuai, WEN Shu-ming, DENG Jian-ying, WU Dan-dan, YANG Jing. Extracting copper from copper oxide ore by a novel zwitterionic reagent and kinetics [J]. International Journal of Minerals, Metallurgy, and Materials, 2015, 22: 241−248.

[12] DENG Jiu-shuai, WEN Shu-ming, YIN Qiong, WU Dan-dan, SUN Quan-wei. Leaching of malachite using 5-sulfosalicylic acid [J]. Journal of the Taiwan Institute of Chemical Engineers, 2016, 71: 20−27.

[13] REVNIVTZEV V I, PUIRIN A M, ARCHANGELSKAYA I N. Flotation separation of minerals of the isomorphous group of feldspars [C]//Proceedings of the 8th International Mineral Processing Congress. Leningrad, Russia, 1968: 1−8.

[14] DEMIR C, BENTLI I, GULGONUL I, CELIK M S. Effects of bivalent salts on the flotation separation of Na-feldspar from K-feldspar [J]. Minerals Engineering, 2003, 16: 551−554.

[15] LIU Wei-jun, ZHANG Shi-qiu, WANG Wei-qing, ZHANG Jie, YAN Wu, DENG Jie, FENG Qi-ming, HUANG Yang. The effects of Ca(II) and Mg(II) ions on the flotation of spodumene using NaOL [J]. Minerals Engineering, 2015, 79: 40−46.

[16] MADEJOVÁ J. Review FTIR techniques in clay mineral studies [J]. Vibrational Spectroscopy, 2003, 31: 1−10.

[17] LU M N, FATAH N, KHODAKOV A. Optimization of solvent free mechanochemical synthesis of Co/Al_2O_3 catalysts using low and high energy processes [J]. Journal of Materials Science, 2017, 52: 12031−12043.

[18] LU Meng-nan, LV Tian-wu, LI Ying, PENG Zheng, GAGNETTA G, SHENG Shou-xiang, HUANG Jun, YU Gang, WEBER R. Formation of brominated and chlorinated dioxins and its prevention during a pilot test of mechanochemical treatment of PCB and PBDE contaminated soil [J]. Environmental Science and Pollution Research, 2017, 6: 1−10.

[19] RAHIMI S, IRANNAJAD M, MEHDILO A. Effects of sodium carbonate and calcium chloride on calcite depression in cationic flotation of pyrolusite [J]. Transactions of Nonferrous Metals Society of China, 2017, 27: 1831−1840.

[20] BUCKLEY A N, HOPE G A, PARKER G K, STEYN J, WOODS R. Mechanism of mixed dithiophosphate and mercaptobenzothiazole collectors for Cu sulfide ore minerals [J]. Minerals Engineering, 2017, 109: 80−97.

[21] WANG P, SU J, DAI W, GERNIGLIARO G, SUN H. Ultrasensitive quartz crystal microbalance enabled by micropillar structure [J]. Applied Physics Letters, 2014, 104: 043504.

[22] BAGGETTO L, DUDNEY N J, VEITH G M. Surface chemistry of metal oxide coated lithium manganese nickel oxide thin film cathodes studied by XPS [J]. Electrochimica Acta, 2013, 90: 135−147.

[23] YIN K, SONG Y X, DONG X R, WANG C, DUAN J A. Underwater superoleophobicity, anti-oil and ultra-broadband enhanced absorption of metallic surface produced by a femtosecond laser: Inspired from fish and chameleon [J]. Scientific Reports, 2016, 6: 36557.

[24] YIN Zhi-gang, SUN Wei, HU Yue-hua, GUAN Qing-jun, ZHANG Chen-hu, GAO Yue-sheng, ZHAI Ji-hua. Depressing behaviors and mechanism of disodium bis (carboxymethyl) trithiocarbonate on separation of chalcopyrite and molybdenite [J]. Transactions of Nonferrous Metals Society of China, 2017, 27: 883−890.

[25] LARSEN E, KLEIV R A. Flotation of quartz from quartz−feldspar mixtures by the HF method [J]. Minerals Engineering, 2016, 98: 49−51.

[26] HACIFAZLIOGLU H, KURSUN I, TERZI M. Beneficiation of low-grade feldspar pre using cyclojet flotation cell, conventional cell and magnetic separator [J]. Physicochemical Problems of Mineral Processing, 2012, 48: 381−392.

[27] ORHAN E C, BAYRAKTAR I. Amine−oleate interactions in feldspar flotation [J]. Minerals Engineering, 2006, 19: 48−55.

[28] VIDYADHAR A, RAO K H. Adsorption mechanism of mixed cationic/anionic collectors in feldspar−quartz flotation system [J]. Journal of Colloid and Interface Science, 2007, 306: 195−204.

[29] VIDYADHAR A, HANUMANTHA RAO K, CHERNYSHOVA I V. Mechanisms of amine−feldspar interaction in the absence and presence of alcohols studied by spectroscopic methods [J]. Colloids and Surfaces A, 2003, 214: 127−142.

[30] SINGH RAMAN P K, AL-SAADI S, HAQUE A. Long-term durability of basalt and glass-fibre reinforced polymer (BFRP/GFRP) bars in seawater and sea sand concrete environment [J]. Construction and Building Materials, 2017, 139: 467−489.

[31] IIISHI K, UMEGAKI Y, TOMISAKA T, KATO T. Force field of K feldspar [J]. Magazine for Crystallography, Crystal Geometry, Crystal Physics, Crystal Chemistry, 1971, 134(3−4): 213−229.

[32] CASEY W H, WESTRICH H R, ARNOLD G W. Surface chemistry of labradorite feldspar reached with aqueous solutions at pH=2, 3, and 12 [J]. Geochimica et Cosmochimica Acta, 1988, 52: 2795−2807.

[33] CARLA M, KORETAKY. Detection of surface hydroxyl species on quartz, γ-alumina, and feldspar using diffuse reflectance infrared spectroscopy [J]. Geochimica et Cosmochimica Acta, 1997, 61: 2193−2210.

[34] WEN Shu-ming, DENG Jiu-shuai, XIAN Yong-jun, LIU Dan. Theory analysis and vestigial information of surface relaxation of natural chalcopyrite mineral crystal [J]. Transactions of Nonferrous Metals Society of China, 2013, 23: 796−803.

自然 pH 条件下 $BaCl_2$ 对钾长石盐酸十二胺浮选的影响

宋 超[1]，周圆圆[1,2]，刘全军[1]，邓建英[1]，李世美[1]，高利坤[1]，余 力[1]

1. 昆明理工大学 国土资源工程学院 复杂有色金属资源清洁利用国家重点实验室，昆明 650093；
2. 郑州航空工业管理学院 机电工程学院 河南省航空材料与应用技术重点实验室，郑州 450046

摘　要：采用浮选试验、吸附量测定、傅里叶转换红外光谱分析(FTIR)以及 X 射线光电子能谱分析(XPS)研究自然 pH 条件下 $BaCl_2$ 对钾长石盐酸十二胺浮选的影响。研究结果表明，低浓度 $BaCl_2$ 对钾长石的浮选具有活化作用，高浓度 $BaCl_2$ 对钾长石浮选具有抑制作用。位于 3548.18、3475.56 和 3414.35 cm^{-1} 的红外光谱谱峰表明盐酸十二胺与钾长石表面作用后有 3 种不同—OH 基团存在。XPS 分析结果表明，Ba^{2+}在钾长石表面吸附后，长石表面 K 原子的浓度降低程度是 Si、Al 和 O 原子的两倍。低浓度下 $BaCl_2$ 的活化作用可归因于矿物表面 K^+和 Ba^{2+}的离子交换作用；高浓度下 $BaCl_2$ 的抑制作用可归因于矿物表面 Ba^{2+}的物理吸附；同时矿浆中 Cl^-浓度的增加也会导致盐酸十二胺溶解平衡的移动，RNH_2H^+的浓度降低。

关键词：钾长石；氯化钡；盐酸十二胺；活化作用；浮选

(Edited by Wei-ping CHEN)